Transport properties of high-angle grain boundaries in Co-doped $YBa_2Cu_3O_{7-\delta}$ thin films

Brian H. Moeckly*
Conductus, Inc., 969 W. Maude Avenue, Sunnyvale, California 94085-2802

Kookrin Char
School of Physics, Center for Strongly Correlated Materials Research, Seoul National University, Seoul 151-742, Korea
(Received 20 August 2001; revised manuscript received 5 February 2002; published 12 April 2002)

We have measured the electrical properties of symmetric 24°-angle grain boundaries in $YBa_2(Cu_{1-x}Co_x)_3O_{7-\delta}$ thin films, for $x=0-0.1$. The Josephson properties of the grain boundaries vary dramatically with the amount of Co doping and with the growth conditions. The critical current decreases and the resistance increases as Co is added until the supercurrent is suppressed. The I_cR_n product scales in a similar manner as other high-T_c weak links. The I-V characteristics become nonlinear with Co doping and often display resonant structure. An analysis of these results indicates that these grain boundaries are not well described by simple models.

DOI: 10.1103/PhysRevB.65.174504 PACS number(s): 74.50.+r, 74.72.Bk, 74.76.Bz, 85.25.Cp

INTRODUCTION

The cause of the Josephson effect in high-angle grain boundaries of $YBa_2Cu_3O_{7-\delta}$ (YBCO) is still not completely understood. Resolution of the puzzle is important because of the need to lessen the deleterious effects of grain boundaries on transport for bulk applications where a high current carrying capability is paramount. Understanding the origin of the Josephson properties is also necessary for furthering the development of a high-T_c junction technology. Already, thin-film high-angle grain boundaries have been instrumental for learning about the physics of high-T_c materials such as the symmetry of the order parameter.[1]

The critical current density (J_c) across in-plane tilt boundaries in YBCO films is suppressed relative to the bulk value, and decreases markedly as the grain boundary angle increases,[2] until the coupling across the boundary is sufficiently weak to give rise to the Josephson effect. In addition to the grain-boundary angle, J_c and R_n of high-angle grain boundaries are also affected by oxygen annealing,[3] ozone annealing,[4] oxygen electromigration,[5] and growth conditions.[6] Phenomenological models have highlighted the role of oxygen content and disorder at the grain boundary.[5] Recent analyses emphasizing the role of the *d*-wave order-parameter symmetry have not fully accounted for the dramatic reduction in J_c with angle;[7] J_c decreases much faster than the *d*-wave symmetry predicts. Grain boundary dislocations may play a role in the transport properties of asymmetric boundaries, but for symmetric boundaries such as the type discussed here, their effect may be benign.[8]

Doping studies are a useful and little-explored complement to the many studies of the effect of varying the grain-boundary angle. Recent investigations of Ca-doped YBCO films have shown that J_c may be increased at low temperature for high-angle grain boundaries which are overdoped by this method,[9,10] prompting excitement in the bulk applications community. We note that Ca-YBCO, when used as a barrier material in superconductor-normal-superconductor junctions, has also played a role in high-T_c Josephson junction development.[11]

While underdoping will not lead to increased J_c values, a study of underdoped grain boundaries may lead to a better understanding of their behavior. It is possible to explore the underdoped region through oxygen reduction. A problem with this technique, however, is that it is quite difficult to uniformly reduce the oxygen content within the YBCO grains, much less at the grain boundaries. We have therefore chosen to explore this effect by studying the transport properties of grain boundaries in Co-doped YBCO films. We expect Co doping to provide a more uniform reduction in the carrier concentration near the grain boundary than oxygen depletion. In this paper we expand on our initial reports.[12]

Co^{3+} substitutes primarily on the Cu(1) oxygen sites in the basal-plane Cu-O chains and causes a reduction in the carrier concentration via charge transfer.[13] Co doping leads to normal-state and superconducting properties which mimic the effect of oxygen depletion quite well,[14,15] even though extra oxygen is assimilated into the structure when Co is added.[16–19] This may be compared to the effect of Ca doping, in which case the Ca^{2+} substitutes on the Y^{3+} sites, and increases the carrier density by introducing one additional hole per substituted ion.[20] Also in contrast to Co-YBCO, Ca-YBCO is known to be oxygen deficient.[21,22] And over time, Ca-YBCO loses more oxygen in order to compensate for the additional charge introduced by Ca doping.[23] This behavior is manifested by an increase in T_c with time.

We have previously studied the transport properties of grain-aligned YBCO thin films that were doped with Co.[24] We found that the transport properties of those films depend strongly on Co content. The bulk J_c value, for example, decreases exponentially with the Co concentration. We also observed that the deposition parameters acutely affect the transport properties, much more so than for undoped films. For laser-ablated films with the same amount of Co, those grown at higher deposition pressure and temperature will have lower T_c values. T_c of a 5% Co-doped YBCO film ($Co/[Co+Cu]=0.05$), for example, may be altered by 40 K

 ©2002 The American Physical Society

simply by changing the deposition pressure from 200 to 800 mTorr. We explained these and other results by assuming that the growth conditions alter the degree to which the Co is either clustered or uniformly distributed throughout the film, thereby altering the length of Cu-O chain fragments in the basal plane and changing the carrier concentration on the superconducting Cu-O_2 planes. We believe that films grown at high pressure have a more uniform distribution of Co than films grown at low pressure. We also think that oxygen in uniformly doped Co-YBCO films is more mobile than in nonuniformly doped samples.

EXPERIMENT

We deposited our Co-YBCO thin films by pulsed laser ablation onto bicrystal $SrTiO_3$ substrates containing a symmetric 24° tilt grain boundary. A 20-nm CeO_2 buffer layer was first deposited in all cases. The deposition rate was 10 Hz, and the laser fluence was 1–1.5 J/cm^2. The targets consisted of $YBa_2(Cu_{1-x}Co_x)_3O_{7-\delta}$, with x varying from 0 to 0.1
(Co/[Co+Cu]=0 to 10%). We employed two sets of deposition parameters for all films. One set of films was grown at a substrate temperature of 800 °C and an oxygen pressure of 800 mTorr, and the other set of films was grown at 780 °C and 200 mTorr. Following deposition to a thickness of 250–300 nm, the films were cooled in 600 Torr of O_2 at 30 °C/min. X-ray-diffraction analysis indicated a complete *c*-axis-normal alignment with no impurity-phase peaks. The films were subsequently photolithographically patterned with Ar-ion etching to form multiple microbridges across the grain boundary with widths of 1, 2, 5, and 10 μm.

R-T CURVES

Figure 1 displays the temperature dependence of the resistance measured across symmetric 24° grain boundaries for bridges with widths of 10 μm. These measurements were taken from films deposited under identical conditions of 800 °C and 800 mTorr with Co contents from 0% to 10%. With increasing Co content, the bulk film resistivity (above T_c) increases, T_c decreases, and the shape of the *R-T* curves changes, as expected.[24] Films deposited at lower temperatures and pressures display less dramatic changes and higher T_c values. At temperatures below the bulk T_c value, there is a ''foot'' on the resistive transition with a resistance corresponding to the grain-boundary resistance, i.e., the R_n value measured from the *I-V* curve. For low Co dopings, the zero-resistance temperature occurs at a temperature lower than T_c. A critical current appears and Josephson behavior occurs below this zero-resistance temperature. For slightly higher Co contents, note that the resistance below T_c increases with decreasing temperature. Such a temperature dependence of the resistance is indicative of some sort of hopping transport mechanism. While we have not studied this temperature dependence in detail, we note that in hopping models the voltage dependence and temperature dependence of the conductance are directly related. We discuss the voltage dependence below. For greater than 5% Co doping, there is no supercurrent at all. For bulk Co-YBCO films, there is a superconducting to insulating crossover for doping levels above 10%,[24] but at the grain boundaries superconductivity is squelched at far lower doping levels. Thus even for Co-doped films, the grain boundary clearly has a deleterious effect.

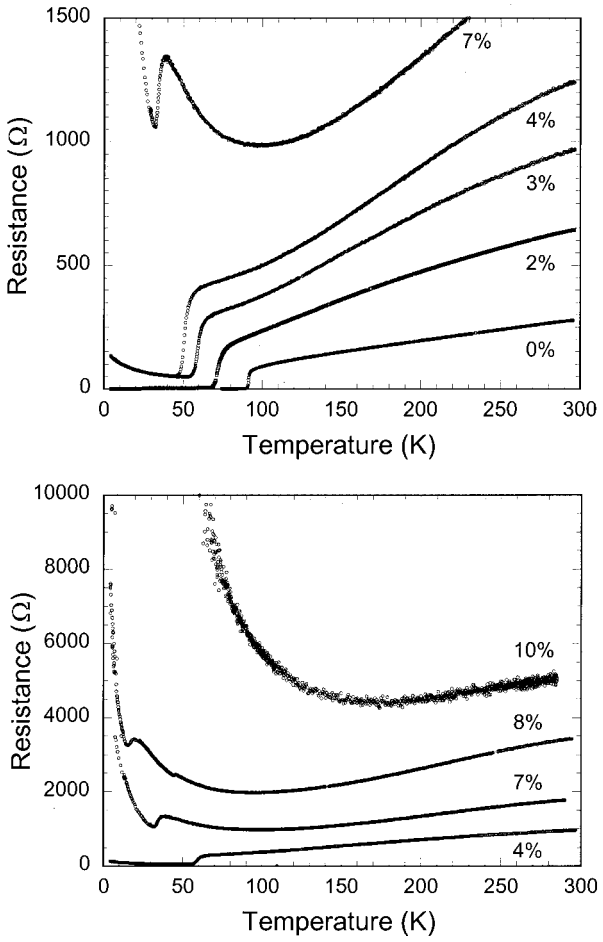

FIG. 1. Temperature dependence of the resistance of Co-doped YBCO microbridges spanning a 24° bicrystal grain boundary. The microbridges are each 10 μm wide and have the Co content listed. Each of these films was deposited at 800 °C and 800 mTorr of O_2, and is between 250 and 300 nm thick. With increasing Co content, the resistance increases, T_c decreases, and the resistance of the grain boundary increases with decreasing temperature.

I-V CHARACTERISTICS

We now examine the *I-V* characteristics of these grain boundary junctions. Figure 2 shows representative *I-V* curves at 4.2 K for Co doping levels of 0%, 3%, and 8%. The microbridge width of these junctions is 10 μm, and the films were all deposited at 800 °C and 800 mTorr. Low-bias plots are shown on the left (to 2 mV), and high-bias plots are shown on the right (to 30 mV). The *I-V* curves are reminiscent of resistively-shunted-junction (RSJ) behavior, and I_c modulates to zero with application of a magnetic field, indicating Josephson coupling. As shown, adding a slight amount of Co strongly affects the *I-V* characteristics: I_c decreases dramatically and R_n increases until by 8% Co doping

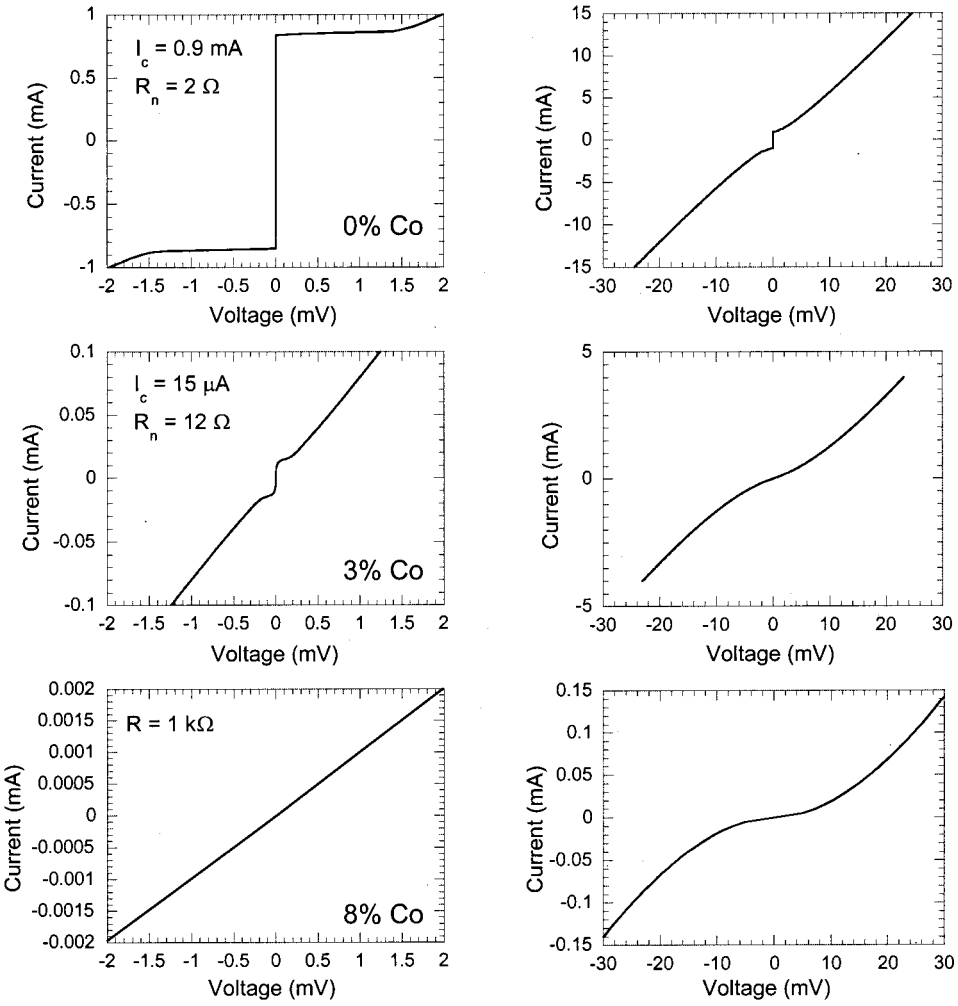

FIG. 2. $I-V$ curves at 4.2 K for bicrystal junctions made with doping levels of 0% (top), 3% (middle), and 8% (bottom). The left column shows low voltage bias plots (to 2 mV), and the right column displays high-bias plots (to 30 mV). As a small amount of Co is added to the YBCO films, I_c decreases rapidly, R_n increases, and the $I-V$ curves become nonlinear at high bias.

there is no detectable supercurrent. Also note that in contrast to the reported behavior for most YBCO grain boundary junctions, the I-V curves become nonlinear at high bias (the conductance increases with voltage bias), so the behavior is clearly not an ideal RSJ response. Furthermore, the bias dependence of the conductance increases as the doping increases. Like the temperature dependence of R_n, this behavior is also suggestive of hopping transport, as we discuss in more detail below.

I_c AND R_n

The measurements of I_c and R_n are summarized in Figs. 3 and 4, which show how the grain boundary J_c and R_nA at 4.2 K depend on Co doping for films grown under different conditions. Figure 3 displays these results for films grown at 800 °C and 800 mTorr. There is a rapid exponential decrease in grain boundary J_c with Co content. There appears to be an increase in J_c for 5% Co doping. This upturn is not understood; the measurements were repeated for three different 5% samples, with the same result each time. Above 5%, there is no detectable critical current for junctions deposited under these conditions. Figure 3(b) displays the R_nA values for the same set of junctions. There is also a strong exponential dependence of R_nA on Co doping, varying by nearly five orders of magnitude up to 10%. Again, there is a slight dip in R_nA at a doping level of 5%, but beyond that R_nA continues to increase steadily. We have pointed out that the I-V curves are nonlinear at high bias, so we note that the R_n values are measured near I_c for the RSJ-like characteristics, and are measured at zero bias for grain boundaries with doping levels above 5% (no I_c). We also note that there is a fair amount of spread in the data, particularly for higher doping levels. This behavior may be caused by increasing inhomogeneity with increased Co doping.[24]

The data are different for Co-YBCO films grown under different deposition conditions. Figure 4 displays the results for films grown at 780 °C and 200 mTorr. As shown in Fig. 4(a), J_c is nearly independent of Co content up to about 3%, although the spread in values does increase. There is a dip in J_c at the 5% level, though the J_c values are nearly an order of magnitude higher than for films grown at higher temperature and pressure. This result supports our earlier observation that grain boundary critical currents are strongly affected by growth conditions. The R_nA values follow a similar trend. As shown in Fig. 4(b), the R_nA values are also virtually constant up to 3%, increasing in value only at a Co level of 5%. We interpret this behavior as indicating that the films grown under these conditions are spatially inhomogeneous compared

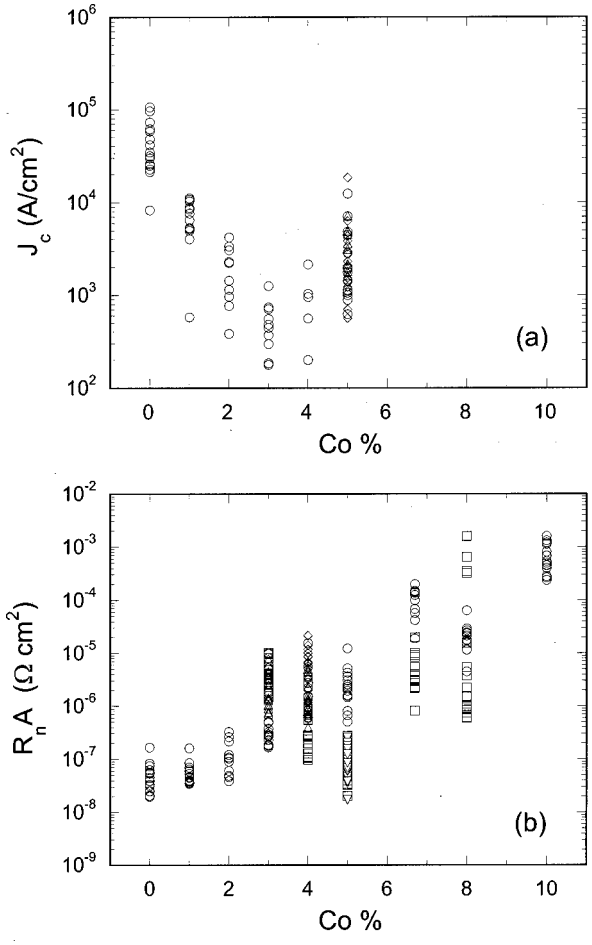

FIG. 3. Critical current density (a) and normalized junction resistance (b) plotted as a function of Co content for several grain boundary weak links grown at 800 °C and 800 mTorr.

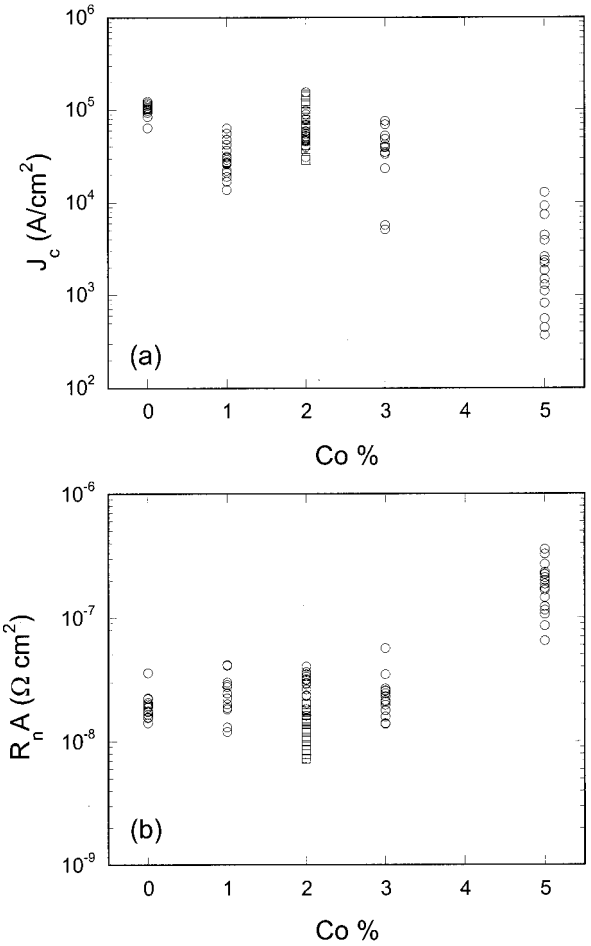

FIG. 4. Critical current density (a) and normalized junction resistance (b) plotted as a function of Co content for several grain boundary weak links grown at 780 °C and 200 mTorr.

to those grown at higher temperature and pressure. If the Co tends to cluster under these conditions, then it is possible that more superconducting paths exist throughout the film and at the grain boundary such that J_c and R_n remain unchanged for low doping levels. It is only for higher doping levels that the superconductive paths become sufficiently disrupted to affect J_c and R_n. These data support the interpretation of our earlier results on bulk Co-doped YBCO films.

I_cR_n SCALING

Like undoped YBCO grain boundaries, the I_cR_n product is not constant, but rather scales as a function of J_c. Figure 5 plots I_cR_n vs J_c for Co-YBCO films grown at (a) high temperature and pressure and (b) lower temperature and pressure. The figure plots data from films having Co contents of 0% to 5%. It can be seen that $I_cR_n \propto J_c^{0.5}$, as found for undoped YBCO grain boundaries.[3,25] Other types of high-T_c weak links also follow a similar scaling relation.[26] However, in this case the variation is caused by changing the Co content, not by changing the grain boundary angle or barrier material. We further observe that the data for the 800/800 films and 780/200 films follow the same trend, though the films grown at lower temperature and pressure have higher I_cR_n products for similar doping levels.

The origin of the scaling behavior for YBCO weak links in general is not precisely determined, so it is difficult to say what is causing the behavior in this case. Certainly it appears not to be due to symmetry considerations, since the grain boundary angle remains the same. We might say that the increased doping acts to increase the effective thickness of the junction barrier, whatever that may be. But since we know that the barrier is not uniform (see below), it is also likely that the effect is to change the number and/or nature of the superconducting and normal current channels across the grain boundary. Whether the scaling behavior is a consequence of the nature of the barrier or of the electrodes, i.e., YBCO, is not yet sorted out.

HIGH-BIAS BEHAVIOR

As stated earlier, we observe that at higher voltage biases the I-V curves become nonlinear, and this nonlinearity increases with Co doping. In fact, we find that there is a power law dependence of I on V, as shown in Fig. 6. This figure plots some examples of normalized conductance (G/A, where $G=I/V$) vs voltage bias V for films grown at (a) high

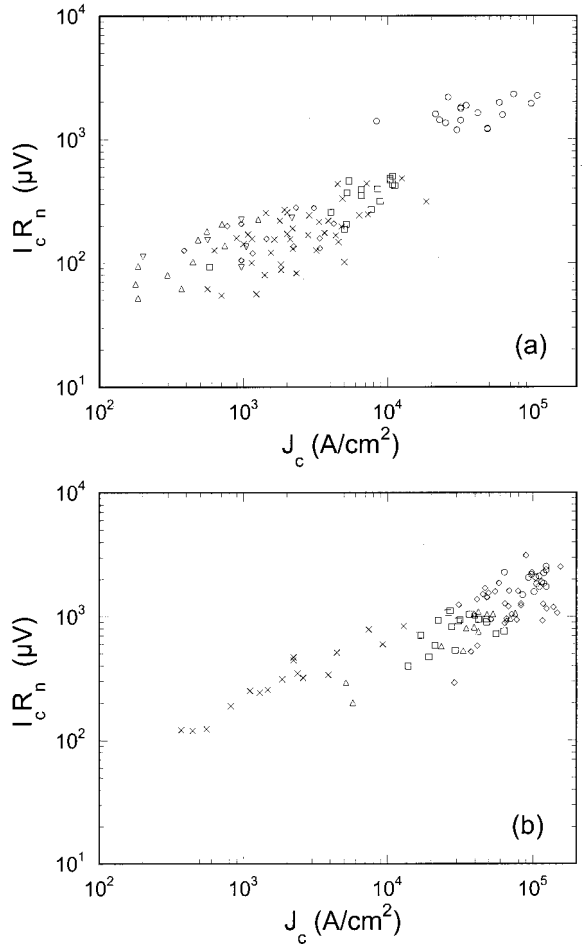

FIG. 5. I_cR_n product of several Co-doped YBCO grain boundary weak links as a function of critical current density for films grown at (a) 800 °C and 800 mTorr and (b) 780 °C and 200 mTorr. The Co content of each film is indicated by the symbol as follows: ○, 0%; □, 1%; ◇, 2%; △, 3%; ▽, 4%; ×, 5%. The I_cR_n product follows the scaling relation $I_cR_n \propto J_c^n$, where (a) $n=0.58$ and (b) $n=0.44$. The data combined produce $n=0.53$.

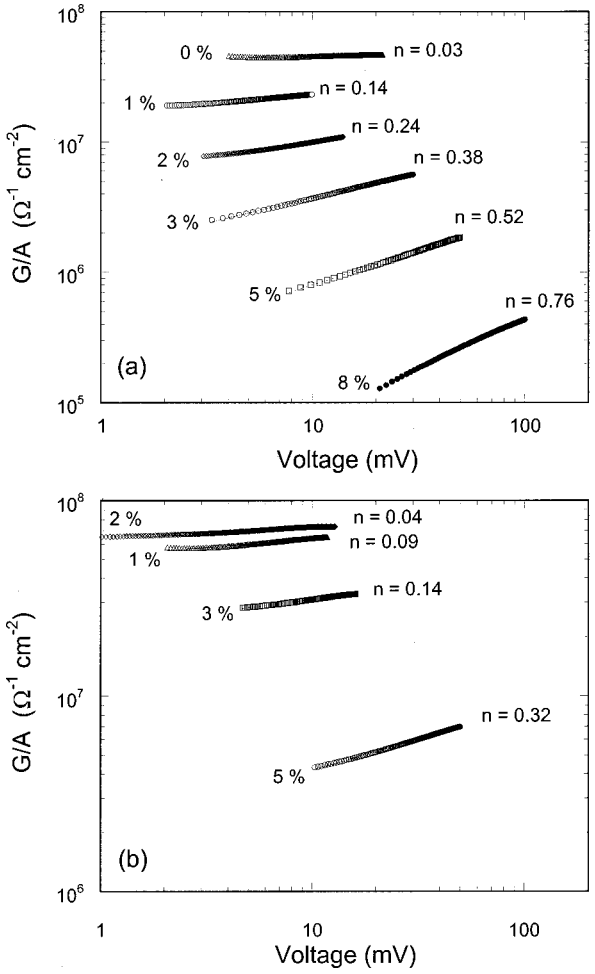

FIG. 6. The normalized conductance ($G=I/V$) vs applied voltage bias V for several Co-doped YBCO grain boundary weak links, grown at (a) 800 °C and 800 mTorr, and (b) 780 °C, and 200 mTorr. The conductance follows a power law $G \propto V^n$. With increasing Co content, the conductance decreases and the nonlinearity of the $I-V$ curve increases.

pressure and temperature and (b) lower pressure and temperature and for various Co doping levels. Note that both the magnitude of the conductance and the dependence on V change with Co doping. This behavior is suggestive of some sort of hopping transport. We find that $G \propto V^n$, with a nearly continuous increase in the power n, as more Co is added. Figure 6(b) shows the results for 780/200 films, in which case the nonlinear behavior is similar, though the magnitude of the conductance is larger for the same Co level, and the nonlinearity is smaller. Also note that for low doping levels, the degree of nonlinearity is similar. These observations are consistent with our picture of these grain boundaries being more inhomogeneous for Co-doped films grown at lower temperature and pressure. We assume that the transport is therefore dominated by a small number of contacts. In this case, changing the Co content does not change the transport through these contacts significantly until higher Co levels are reached.

This general behavior is vaguely reminiscent of studies of Nb junctions with amorphous silicon barriers.[27] Similar power laws were observed in that case, and it was demonstrated that the conductance followed the Glazman-Matveev prediction[28] for hopping conduction through localized states. However, the conductance we observe is much less than for the a-Si barriers, and our $G(V)$ data does not neatly fit resonant tunneling models. Since the density of localized states for a-Si is already quite high, this again may suggest that we are observing the effect of parallel channels of different conductivity. Adding Co may then alter the proportion of superconducting (direct channels) and normal channels. Co addition may also change the conductivity of these channels by altering the density of localized states or by changing the carrier concentration.

I-V STRUCTURE

We have observed clear structure in the low-temperature I-V characteristics of more than 90 of our Co-YBCO grain boundary junctions (out of 414 junctions measured). This structure occurs primarily for junctions with high-J_c values

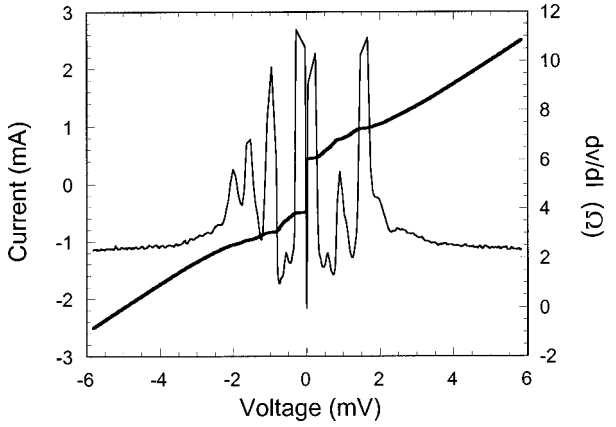

FIG. 7. An example of the resonant structure inherent in the I-V characteristics of many Co-doped YBCO grain boundary weak links. The structure is most prominent for weak links with higher J_c values, and for those grown at 780 °C and 200 mTorr. This curve is from a 10-μm-wide weak link grown at 800 °C and 800 mTorr.

(R_n for these junctions is always high relative to undoped YBCO grain boundaries). An example of such an I-V characteristic is shown in Fig. 7. Similar structure observed in wide, high-R_n undoped YBCO grain boundary weak links has been attributed to the existence of Fiske mode resonances.[29] In that case, the grain boundary is modeled as a uniform tunnel junction in which resonances arise due to interference of the Josephson oscillations with the reflection of electromagnetic waves in the barrier. We have analyzed our data in terms of the Fiske mode picture, in which the position of the Fiske peaks is given by $V_n = n\Phi_0 \nu/2w$, where w is the junction width and ν is the mode velocity given by $\nu = c[d/\mu_r \varepsilon_r (2\lambda + d)]^{1/2}$. Here c is the speed of light, λ is the penetration depth, and u_r is the relative permeability taken to be unity. We can therefore extract d/ε_r, the ratio of barrier thickness to dielectric constant. From this value we can derive a barrier capacitance, since $d/\varepsilon_r = A\varepsilon_0/C$, where A is the cross sectional area. The result is plotted in Fig. 8(a) as a function of the width. To compute these values, we assumed a penetration depth equal to 140 nm; using slightly different values will affect the results by only small factors. The result of the Fiske analysis is that the *calculated* C/A value varies markedly with width; this variation is *unphysical*. It is important to note that other measurable properties such as J_c and R_nA do not change with width, so the grain boundary properties do indeed appear to remain constant with width. To make this point further, we can use this calculated (not actual) value of C/A to compute the expected McCumber parameter β_c, given by $\beta_c = 2\pi I_c R_n^2 C/\Phi_0$, which should be consistent with the amount of hysteresis seen in the I-V characteristics. The result of this computed β_c vs width is shown in Fig. 8(b). We do not observe any hysteresis in any of the I-V characteristics of our Co-YBCO grain boundaries. So, from the plot, we see that the analysis appears to be reasonable for some of the junctions, particularly those of larger widths, but for smaller widths, the result is again unphysical, since β_c should be less than 1; we see that the computed value is orders of magnitude too high.

The point of Fig. 8 is thus to show that the Fiske model

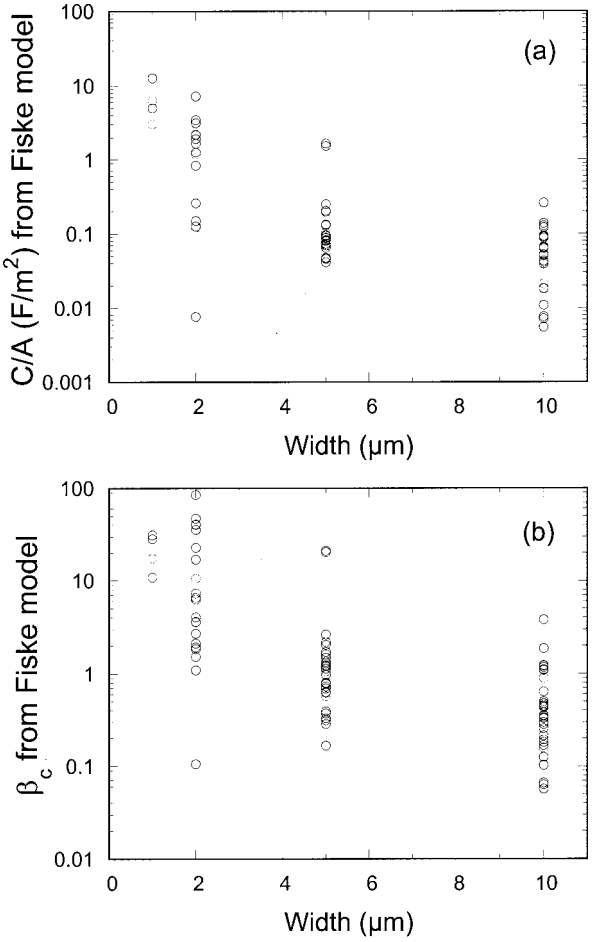

FIG. 8. The width dependence of (a) the normalized capacitance and (b) the McCumber parameter which are computed based upon a Fiske mode analysis of the resonant structure found in many of our Co-doped YBCO grain boundary weak links. If the Fiske mode analysis is correct, these quantities should be independent of the junction width, which they are not. Therefore, interpretation of the I-V structure in terms of Fiske mode peaks cannot be correct.

cannot successfully describe the I-V structure of these grain boundary junctions. While it is possible to choose a value of λ such that the computed Fiske capacitance matches the I-V hysteresis for some junctions, it is clear that over a wide range of junction parameters, this analysis breaks down. In addition, for most high-T_c junctions, C/A (computed from the I-V hysteresis) scales with R_nA.[30–32] However, for these Co-YBCO junctions, we find no such scaling relation using the C/A value computed from Fiske analysis, again indicating that this analysis is likely not correct. In summary, we find that it is not possible for narrow YBCO grain boundary junctions to support Fiske mode resonances. Therefore, the structure in the I-V characteristics must be due to something else.

Resonant modes may also arise in a different region of parameter space, specifically for junctions with large values of inductance and capacitance. This is the so-called ''beating mode'' picture derived from analysis of the dc superconducting quantum interference device (SQUID).[33,34] This may imply that the resonance modes we observe are due to strong

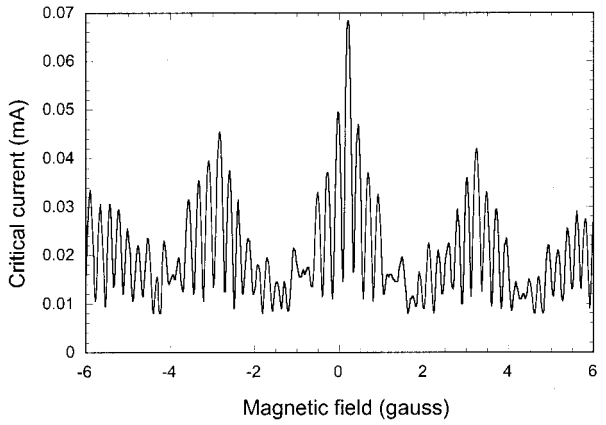

FIG. 9. A striking example of the 4.2-K magnetic-field diffraction pattern of a 1% Co-doped grain boundary weak link that is 10 μm wide. A pattern similar to this is expected if two 2-μm-wide weak links are separated by a distance of 10 μm. Such patterns demonstrate the inhomogeneity of many grain boundary weak links.

junction inhomogeneities. The fact that we observe significantly more structure in the I-V characteristics of grain boundaries grown at lower temperature and pressure may support this view, given that we believe that these Co-YBCO films are more inhomogeneous. The conditions for the junctions to support beating mode resonances are those of sufficient inductance and capacitance, such that $\beta_L \equiv LI_c/\Phi_0 \geqslant 3/2$ and $1 \leqslant \beta_C \leqslant \pi\beta_L$. It is interesting that we observe an I-V structure for junctions with higher I_c values, perhaps indicating sufficient β_L values to satisfy this picture. This picture also implies that these junctions contain significant inductance which is not usually recognized in the analysis of wide junctions, and only becomes apparent when the junction width is narrow.

MAGNETIC-FIELD DEPENDENCE

It is not possible to check whether the beating mode picture is correct, though we can offer evidence to support the idea of inhomogeneities at the grain boundaries. We often observe nonideal $I_c(H)$ diffraction patterns, particularly for *narrow* junctions. A striking example is shown in the $I_c(H)$ diffraction pattern displayed in Fig. 9, which is taken from a 10-μm-wide junction. This pattern in fact is reminiscent of a dc SQUID, with two apparent periodicities, one being due to the size of the junction and the other due to two Josephson contacts. This pattern can be described by two superconducting filaments of width 2 μm each spaced 10 μm apart.

SUMMARY

A look at the variety of data we have presented convinces us that the transport properties of these high-angle grain boundaries cannot be described by assuming an ideal tunnel barrier between *d*-wave superconducting electrodes. Since the angle of all our tilt boundaries is fixed, the symmetry of the wave function in the electrodes has no direct bearing on the trends we report. It is also clear that the picture of an ideal tunnel barrier between electrodes of varying T_c does not describe our data. We do see a reduction in T_c of the electrodes as Co is added to the YBCO. For tunnel junctions the I_cR_n product should depend only on T_c of the electrodes, but this is not the case; the junction properties deteriorate much faster than those of the electrodes. While there remains a significant bulk film T_c for Co dopings greater than 5%, for example, the grain boundary critical current abruptly disappears for these higher doping levels. Thus doping the YBCO films with Co also degrades the properties of the grain boundaries, not just the grains themselves. We do not believe that Co migrates preferentially to the grain boundaries, however. We have previously shown[24] that Co-YBCO films grown at high temperature appear to be uniform. This finding suggests that Co migration is not significant at our growth temperatures, and the mobility of Co does not seem to be sufficient for the Co atoms to migrate preferentially to the grain boundaries. If the properties of the grain boundaries are then largely determined by oxygen disorder, adding Co appears to increase this disorder. (There is no reason to believe the spatial uniformity of Co to be worse at the grain boundary, since inspection typically shows good cation crystalline order of YBCO grain boundaries.) The thin-film growth conditions, however, also affect the film and grain-boundary properties, so we believe that the properties of the grain boundary are driven by disorder.

These ideas are also supported by examining the temperature dependence of the junction R_n values. As we have shown, the value of R_n and its temperature dependence are significantly altered with Co doping and growth conditions. If the Josephson properties are determined by tunneling, this resistance should be independent of temperature or the properties of the electrodes.

High-T_c grain boundaries have also been conjectured to contain a significant number of localized states.[35,36] Such models purport to explain the I_cR_n scaling which we have mentioned, since it is incompatible with an ideal tunnel junction picture. If, however, the number of these localized states are decreased by adding Co, then we should move to the tunneling picture with Co addition, which appears not to be the case: R_n remains far too low even as I_c quickly goes to zero. Alternatively, if we imagine the number of localized states to be increased by Co doping, then we would expect R_n to decrease, which it does not. A more complex picture must govern the behavior we observe.

We have also demonstrated how the tunneling picture cannot cleanly explain the I-V structure we observe over the large range of junction properties that we present. A narrow tunnel junction cannot support such electromagnetic resonances. We believe that the model of YBCO grain boundaries consisting of a number of superconducting connections has merit in explaining our data. In this picture, we can imagine that the effect of Co doping is to suppress the superconductivity of these connections, essentially shutting off superconducting contacts as Co is added. This can explain the increasing inhomogeneity of the grain boundaries as the amount of Co is increased. A quick reduction in superconducting current paths is then accompanied by an increasing number of nonlinear resistive paths, which is consistent with the data we have presented.

We have shown how the Josephson properties of high-angle YBCO grain boundaries change with Co doping and

growth conditions. These results emphasize that the interfaces in these materials remain of prime importance, and that the transport properties across these interfaces are more complicated than a picture comprised of grains of *d*-wave symmetry separated by a simple tunnel barrier.

ACKNOWLEDGMENTS

This work was supported in part by the Naval Research Laboratory and the Office of Naval Research, Contract No. N00014-96-C-2095.

*Electronic address: moeckly@conductus.com

[1] C. C. Tsuei, J. R. Kirtley, C. C. Chi, L. S. Yu-Jahnes, A. Gupta, T. Shaw, J. Z. Sun, and M. B. Ketchen, Phys. Rev. Lett. **73**, 593 (1994).
[2] D. Dimos, P. Chaudhari, and J. Mannhart, Phys. Rev. B **41**, 4038 (1990).
[3] S. E. Russek, D. K. Lathrop, B. H. Moeckly, R. A. Buhrman, D. H. Shin, and J. Silcox, Appl. Phys. Lett. **57**, 1155 (1990).
[4] M. Kawasaki, P. Chaudhari, and A. Gupta, Phys. Rev. Lett. **68**, 1065 (1992).
[5] B. H. Moeckly, D. K. Lathrop, and R. A. Buhrman, Phys. Rev. B **47**, 400 (1993).
[6] K. Char, M. S. Colclough, S. M. Garrison, N. Newman, and G. Zaharchuk, Appl. Phys. Lett. **59**, 733 (1991).
[7] H. Hilgenkamp, J. Mannhart, and B. Mayer, Phys. Rev. B **53**, 14 586 (1996).
[8] N. D. Browning, J. P. Budan, P. D. Nellist, D. P. Norton, M. F. Chisholm, and S. J. Pennnycook, Physica C **294**, 183 (1998).
[9] A. Schmehl, B. Goetz, R. R. Schultz, C. W. Schneider, H. Bielefeldt, H. Hilgenkamp, and J. Mannhart, Europhys. Lett. **47**, 110 (1999).
[10] G. Hammerl, A. Schmehl, R. R. Schultz, B. Goetz, H. Bielefeldt, C. W. Schneider, H. Hilgenkamp, and J. Mannhart, Nature (London) **407**, 162 (2000).
[11] L. Antognazza, B. H. Moeckly, T. H. Geballe, and K. Char, Phys. Rev. B **52**, 4559 (1995).
[12] B. H. Moeckly and K. Char, Bull. Am. Phys. Soc. **42**, 64 (1997).
[13] J. Clayhold, N. P. Ong, Z. Z. Wang, J. M. Tarascon, and P. Barboux, Phys. Rev. B **39**, 7324 (1989).
[14] M. Kakihana, S.-G. Eriksson, L. Börjesson, L.-G. Johansson, C. Ström, and M. Köll, Phys. Rev. B **47**, 5359 (1993).
[15] A. Carrington, A. P. Mackenzie, C. T. Lin, and J. R. Cooper, Phys. Rev. Lett. **69**, 2855 (1992).
[16] C. Y. Yang, A. R. Moodenbaugh, Y. L. Wang, Y. Xu, S. M. Heald, D. O. Welch, M. Suenaga, D. A. Fischer, and J. E. Penner-Hahn, Phys. Rev. B **42**, 2231 (1990).
[17] P. Zolliker, D. E. Cox, J. M. Tranquada, and G. Shirane, Phys. Rev. B **38**, 6575 (1988).
[18] Y. K. Tao, J. S. Swinnea, A. Manthiram, J. S. Kim, J. B. Goodenough, and H. Steinfink, J. Mater. Res. **3**, 248 (1988).
[19] J. M. Tarascon, P. Barboux, P. F. Miceli, L. H. Greene, and G. W. Hull, Phys. Rev. B **37**, 7458 (1988).
[20] H. M. Appelboom, H. Sato, and M. Naito, Physica C **221**, 125 (1994).
[21] G. Xiao and N. S. Rebello, Physica C **211**, 433 (1993).
[22] A. Manthiram and J. B. Goodenough, Physica C **159**, 760 (1989).
[23] J. T. Kucera and J. C. Bravman, Phys. Rev. B **51**, 8582 (1995).
[24] B. H. Moeckly and K. Char, Physica C **265**, 263 (1996).
[25] G. Deutscher and P. Chaudhari, Phys. Rev. B **44**, 4664 (1991).
[26] B. H. Moeckly, in *Advances in Superconductivity XI*, edited by N. Koshizuka and S. Tajima (Springer-Verlag, Tokyo, 1999), Vol. 2, p. 1141.
[27] Y. Xu, D. Ephron, and M. R. Beasley, Phys. Rev. B **52**, 2843 (1995).
[28] L. I. Glazman and K. A. Matveev, Zh. Eksp. Teor. Fiz. **94**, 332 (1988) [Sov. Phys. JETP **67**, 1276 (1988)].
[29] D. Winkler, Y. M. Zhang, P. A. Nilsson, E. A. Stepantsov, and T. Claeson, Phys. Rev. Lett. **72**, 1260 (1994).
[30] B. H. Moeckly and R. A. Buhrman, Appl. Phys. Lett. **65**, 3126 (1994).
[31] B. H. Moeckly and R. A. Buhrman, IEEE Trans. Appl. Supercond. **5**, 3414 (1995).
[32] P. F. McBrien, R. H. Hadfield, W. E. Booij, A. Moya, F. Kalhmann, M. G. Blamire, C. M. Pegrum, and E. J. Tarte, Physica C **339**, 88 (2000).
[33] Y. Imry and P. M. Marcus, IEEE Trans. Magn. **MAG-13**, 868 (1977).
[34] E. Ben-Jacob and Y. Imry, J. Appl. Phys. **52**, 6806 (1981).
[35] J. Halbritter, Phys. Rev. B **46**, 14 861 (1992).
[36] A. Marx, U. Fath, L. Alff, and R. Gross, Appl. Phys. Lett. **67**, 1929 (1995).